



SAFETY MARGIN EVALUATION BASED ON INCREMENTAL DYNAMIC ANALYSIS OF SEISMICALLY ISOLATED BUILDINGS

Y. Izawa ⁽¹⁾, Y. Koyama ⁽²⁾, M. Kobayashi ⁽³⁾

⁽¹⁾ Senior Project Engineer, Structural Engineering Dept., NIHON SEKKEI, INC., izawa-y@nihonsekkei.co.jp

⁽²⁾ Graduate Student, Meiji University, ce183014@meiji.ac.jp

⁽³⁾ Professor, Meiji University, masahito@meiji.ac.jp

Abstract

This paper shows that the safety margin of seismically isolated buildings against input ground motions exceeding the design assumption is evaluated by incremental dynamic analysis. The effect of the difference of the superstructure models on the safety margin of seismically isolated buildings is analyzed. In incremental dynamic analysis, 16 sets of 32 ground motion groups are used to verify the safety margin of seismically isolated buildings. The superstructure of the analysis models are 3 cases: a moment frame, a shear wall is placed in the lower story of the superstructure, and a multi-story shear wall is placed in the entire story of the superstructure. In conclusion, if large deformation of seismic isolation layer is acceptable, it is effective for improving the safety margin to arrange the seismic elements in the entire building in a well-balanced manner like multi-story shear walls.

Keywords: seismic isolation, incremental dynamic analysis, safety margin

1. Introduction

In recent years, it has become clear that an excessive response occurs in seismically isolated buildings (SIBs) due to long-period and long-duration ground motions or pulse-like ground motions. When SIBs reach a certain limit that exceeds the design assumptions, the damage increases rapidly and reaches its ultimate state. Therefore, SIBs have low redundancy against input ground motions exceeding the design assumption (extreme ground motions).

In SIBs, excessive deformation of seismic isolation layer causes collision to the moat walls and hardening of laminated rubber bearings. These cause an excessive response of the superstructure, and yielding is inevitable. Kikuchi et al. have conducted a basic study on the effect of yielding of the superstructure on SIBs on the seismic response [1]. However, in the design of SIBs, it is generally not allowed the superstructure to yield. Therefore, enough consideration has not been made as to how much safety margin is secured in the superstructure of SIBs.

FEMA P695 shows a method for probabilistically evaluating the seismic safety of buildings up to the ultimate state using multiple ground motions and incremental dynamic analysis (IDA). This method evaluates the seismic safety by evaluating probabilistically the level of ground motion that reaches the ultimate state while gradually increasing the ground motion magnification selected under certain conditions. Qu et al. and Nakazawa et al. have studied influence of isolation gap size on the collapse performance of SIBs using IDA [2-3].

This paper shows that the safety margin of SIBs against extreme ground motions is evaluated by IDA. The effect of the difference of the superstructure models on the safety margin of SIBs is analyzed.

2. Analysis Models

The analysis model used for IDA is an 11-story reinforced concrete base-isolated structure. The analysis models are designed based on the design criteria commonly used in Japan. The frame type of the superstructure is changed. The isolation devices are natural rubber bearings (NRBs) and steel dampers (SDs).



2.1 Structural Design

In the design of SIBs in Japan, designer sets design criteria to ensure the performance of building, and time history response analysis confirms that this is satisfied [4]. The design criteria are set for the rare ground motion level and the extremely rare ground motion level. The design input ground motions used in the time history response analysis are observation ground motions, notification ground motions, and site ground motions. The notification ground motions are artificial ground motion created to match the target spectrum set by notification of the Ministry of Construction.

Table 1 shows design criteria of analysis models for the extremely rare ground motions in this paper. The design shear force is set to envelop the response shear force in consideration of the variation of the isolation devices. The vertical stress of NRBs is considered the design seismic intensity 0.3G for the long-term axial force as the effect of vertical ground motion.

Table 1 – Design criteria of analysis models for extremely rare ground motions in this paper

Input level	Extremely rare ground motions
<i>Superstructure</i>	
Stress occur in main member	Short-term allowable stress or less
Inter-story drift angle	1/100 or less
<i>Isolation Device (Natural Rubber Bearing)</i>	
Shear strain	200% [40cm] or less
<i>Vertical stress</i>	
Compression	2 times or less of standard stress
Tension	1.0 N/mm ² or less

Table 2 shows design input ground motions for the extremely rare ground motions. The maximum velocity of the observation ground motion is normalized to 50 cm/s. The bottom of the foundation can be regarded as the engineering bedrock, and the notification ground motions do not consider the amplification of the surface ground.

Table 2 – Design input ground motions

Type	Ground Motion [Phase characteristics in notification ground motion]	Maximum acceleration [cm/s ²]	Duration [s]
Observation ground motion	El Centro 1940 NS	510.8	60
	Taft 1952 EW	496.6	60
	Hachinohe 1968 NS	333.4	60
Notification ground motion	Random phase	372.0	120
	Hachinohe 1968 NS phase	393.3	350
	JMA-Kobe 1995 NS phase	378.9	120

In the structural design of the analysis models, manufacturing errors and variations due to aging of the isolation devices is considered. The stiffness of NRB is assumed to vary from -15% to + 25%, and the stiffness and yield load of SD are assumed to vary from -10% to + 10%.

2.2 Superstructure

The plane shape of the analysis model is a 36.0 m × 36.0 m composed of 4 spans of 9.0 m. The height of seismic isolation layer is 3.0 m, the height of ground floor is 4.0 m, and the height from first floor is 40.0 m. The superstructure of the analysis models are 3 cases: a moment frame (moment frame model, MFM), a shear wall is placed in the lower story of the superstructure (lower story shear wall frame model, LWM), and a multi-story shear wall is placed in the entire story of the superstructure (multi-story shear wall frame model, MWM). The analysis is only in the X direction. Table 3 shows building specifications of analysis models, Fig. 1 shows floor plan, and Fig. 2 shows framing elevation of line Y2.



Table 3 – Building specifications of analysis models

Analysis model	Moment frame model (MFM)	Lower story shear wall frame model (LWM)	Multi-story shear wall frame model (MWM)
Floor	10	10	10
Structure type	Reinforced concrete	Reinforced concrete	Reinforced concrete
Frame type	Moment frame	Shear wall frame	Shear wall frame
Total weight [kN]	198,500	199,900	202,300
Materials			
Concrete	Fc42 (1~7F), Fc36 (8~RF)	Fc42 (1~7F), Fc36 (8~RF)	Fc42 (1~7F), Fc36 (8~RF)
Main bar	SD390(D32)	SD390(D32)	SD390(D32)
Wall reinforcement	-	SD295A (D16)	SD295A (D13, D16)
Shear reinforcement	SD295A (D13)	SD295A (D13), SPR785 (H13)	SD295A (D13), SPR785 (H13)
Member sections			
Column (Wide×Depth) [mm]	800×800, 850×850, 900×900, 950×950	800×800, 850×850, 900×900, 950×950	800×800, 850×850, 900×900, 950×950
Girder (Wide×Depth) [mm]	600×900~650×950, 650×1,800	600×900~650×950, 650×1,800	600×900~650×950, 650×1,800
Wall (Thickness) [mm]	-	300	180, 200, 300

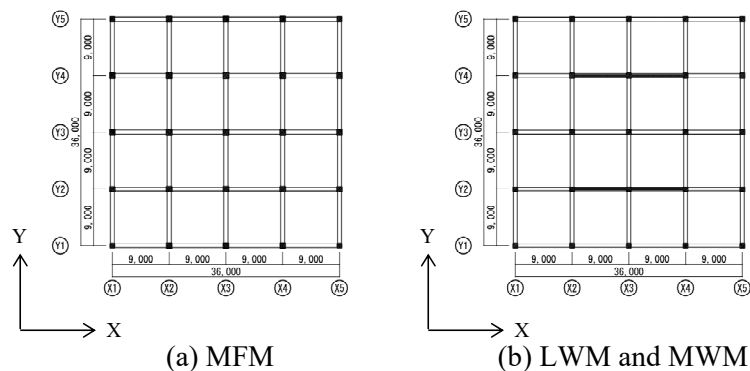


Fig. 1 – Floor plan

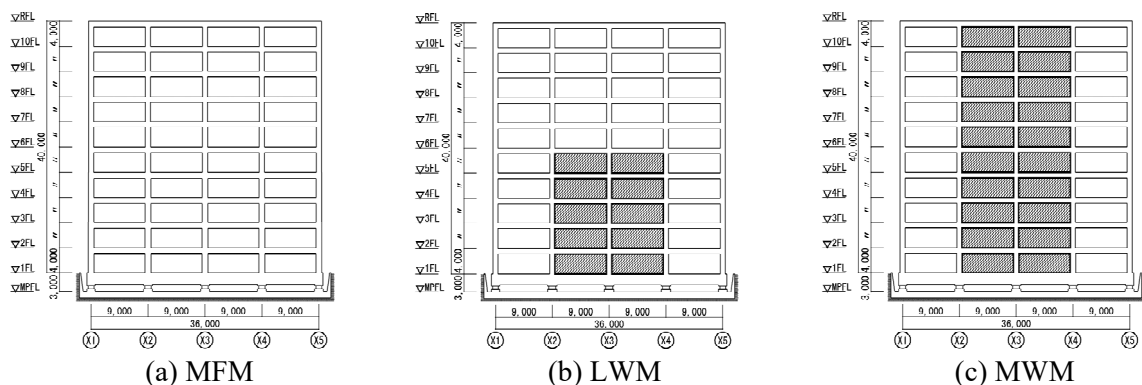


Fig. 2 – Framing elevation of line Y2

2.3 Isolation Devices

The isolation devices are NRBs and SDs. Fig. 3 shows isolation devices layout. Table 4 and Table 5 show specifications of NRBs and SDs, respectively.

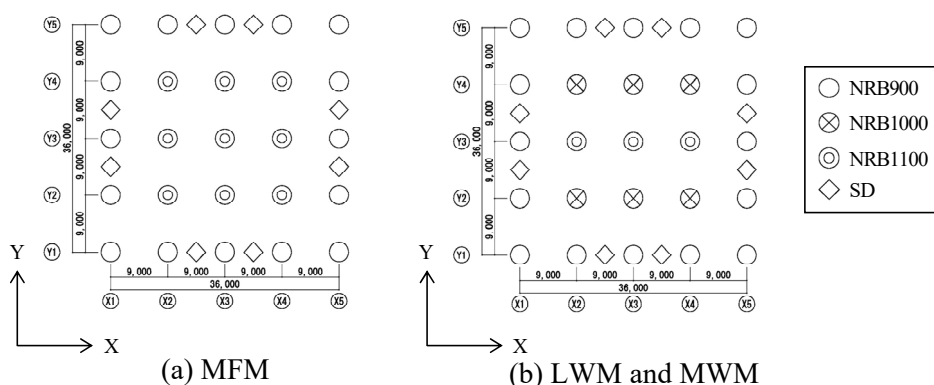


Fig. 3 – Isolation devices layout

Table 4 – Specifications of natural rubber bearings

Symbol	NRB900	NRB1000	NRB1100
<i>Number</i>			
MFM	16	9	-
LWM	16	3	6
MWM	16	3	6
Outer diameter [mm]	900	1,000	1,100
Shear modulus [N/mm ²]	0.39	0.39	0.39
Total thickness of rubber [mm]	197.2	203.0	203.0
Primary shape factor	35.8	33.2	36.8
Secondary shape factor	4.6	4.9	5.4
Standard stress [N/mm ²]	12	15	15
Vertical stiffness [kN/m]	3,565,000	4,003,000	5,308,000
Critical strain [%]	400	400	400

Table 5 – Specifications of steel dampers

Symbol	SD
<i>Number</i>	8
Initial stiffness [kN/m]	19,200
Post-yield stiffness [kN/m]	320
Total thickness of rubber [mm]	203.0
Yield load [kN]	608
Critical deformation [mm]	850

The restoring force characteristics of NRB consider hardening. According to the example of hardening characteristics of NRB indicated in the recommendation for design of SIBs in Japan, it shows linearity up to a shear strain of 250%, 2 to 3.75 times the initial stiffness at 250 to 350%, and 5.5 to 8.75 times the initial stiffness after 350% [5]. Based on this, the hardening characteristic of NRB is set to 2 times the initial stiffness at 50 to 70 cm and 7 times at 70 cm or more. Fig. 4 shows restoring force characteristic of NRB. The hysteretic characteristic of NRB is nonlinear elasticity. The restoring force characteristic of SD is the normal bi-linear as shown in Fig. 5.

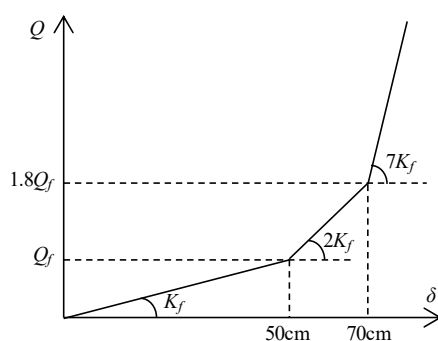


Fig. 4 – Restoring force characteristic of natural rubber bearing

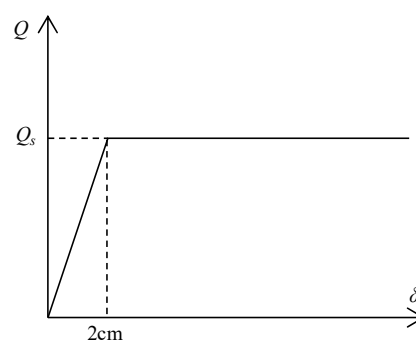


Fig. 5 – Restoring force characteristic of steel damper

2.4 Incremental Dynamics Analysis

IDA is performed using an 11-mass bending-shear model. Static load incremental analysis is performed on the three-dimensional frame model using the design shear force distribution. The bending deformation component is elastic. The skeleton curve is modeled as a three-fold line to approximate the load-deformation



relationship of the shear deformation component. The hysteretic characteristic of the superstructure is Takeda model. The starting point of the ductility factor is the deformation at the time when the plastic hinge is first generated in the members constituting the layer.

IDA is performed by the Newmark- β method, $\beta = 0.25$. The damping is proportional to the momentary stiffness, and the damping factor is 0.03 for the fundamental natural period when the seismic isolation layer is fixed. The damping of the seismic isolation layer is not considered. Here, the hardening of NRB is used without considering the collision to the moat walls.

3. Ground Motion Group

In this paper, nonlinear time-history response analysis on the ground motion group is performed. The response of the structure by IDA which gradually increases the ground motion magnification is grasped continuously, and the safety margin against the criteria such as collapse is evaluated. This method is summarized in FEMA P695 [6]. The selection of ground motions is based on FEMA P695. The selection method of ground motions, the normalization method of ground motions, and the scaling method of the ground motion magnification is outlined.

3.1 Ground Motion Record Set in FEMA P695

The ground motion group used in this paper is the Far-Field ground motion record set shown in FEMA P695. However, since 8 ground motions with a maximum effective period of less than 6 seconds are not suitable for the evaluation of SIBs, 16 sets of 32 ground motions are used except for 6 sets including this ground motion [2-3]. Table 6 shows ground motion record set.

Table 6 – ground motion record set

No. (FEMA ID No.)	Observation record				Original data				
	Date	Name (Country)	Epicenter distance [km]	Magnitude	Componet	Lowest Usable Freq. [Hz]	PGA [cm/s ²]	PGV [cm/s]	NM_i
1 (2)	1/17/1994	Northridge (USA)	26.5	6.7	LOS000	0.06	402.1	43.0	0.94
					LOS270	0.13	472.7	45.2	0.89
2 (3)	11/12/1999	Duzce (Turkey)	41.3	7.1	BOL000	0.06	713.5	56.5	0.71
					BOL090	0.06	806.5	62.1	0.65
3 (4)	10/16/1999	Hector Mine (USA)	26.5	7.1	HEC000	0.03	260.4	28.5	1.41
					HEC090	0.04	330.3	41.8	0.96
4 (5)	10/15/1979	Imperial Valley (USA)	33.7	6.5	H-DLT262	0.06	233.2	26.0	1.55
					H-DLT352	0.06	344.3	33.0	1.22
5 (7)	1/16/1995	Kobe (JAPAN)	8.7	6.9	NIS000	0.13	499.5	37.3	1.08
					NSI090	0.13	493.0	36.7	1.10
6 (8)	1/16/1995	Kobe (JAPAN)	46.0	6.9	SHI000	0.13	238.5	37.8	1.06
					SHI090	0.10	207.8	27.9	1.44
7 (10)	8/17/1999	Kocaeli (Turkey)	53.7	7.5	ARC000	0.09	214.6	17.7	2.27
					ARC090	0.05	147.0	39.6	1.02
8 (11)	6/28/1992	Landers (USA)	86.0	7.3	YER270	0.07	344.5	51.5	0.78
					YER360	0.07	240.1	29.8	1.35
9 (12)	6/28/1992	Landers (USA)	82.1	7.3	CLW-LN	0.13	277.4	25.6	1.57
					CLW-TR	0.13	408.8	42.3	0.95
10 (14)	10/18/1989	Loma Prieta (USA)	31.4	6.9	G03000	0.13	544.3	35.7	1.13
					G03090	0.13	360.3	44.7	0.90
11 (15)	6/20/1990	Manjil (Iran)	40.4	7.4	ABBAR-L	0.13	504.6	43.2	0.93
					ABBAR-T	0.13	486.8	53.1	0.74
12 (16)	11/24/1987	Superstition Hills (USA)	35.8	6.5	B-ICC000	0.13	350.9	46.4	0.87
					B-ICC090	0.13	253.3	40.9	0.98
13 (18)	4/25/1992	Cape Mendocino (USA)	22.7	7.0	RIO270	0.07	378.0	44.0	0.92
					RIO360	0.07	538.3	42.1	0.96
14 (19)	9/20/1999	Chi-Chi (Taiwan)	32.0	7.6	CHY101-E	0.04	346.1	70.6	0.57
					CHY101-N	0.05	431.6	115.0	0.35
15 (20)	9/20/1999	Chi-Chi (Taiwan)	77.5	7.6	TCU045-E	0.03	465.2	36.7	1.10
					TCU045-N	0.05	502.1	29.1	1.03
16 (22)	5/6/1976	Friuli (Italy)	20.2	6.6	A-TMZ000	0.13	344.5	22.0	1.83
					A-TMZ270	0.13	308.7	30.8	1.31



3.2 Normalization Method of Ground Motions

Unlike the FEMA P695, the normalization method for ground motion groups adopts a method that matches the median of PGV of 32 ground motions. Like Qu et al. and Nakazawa et al., the normalization factor of the i -th ground motion NM_i is as follows:

$$NM_i = \text{median}(\text{PGV}_i) / \text{PGV}_i \quad (1)$$

where PGV_i is PGV of the i -th ground motion. For all ground motions after the normalization, the maximum velocity coincides with the median [2-3].

3.3 Scaling Method of Ground Motion Group

In FEMA P695, the ground motion group is scaled using the acceleration response spectrum value, $S_a(T_1)$, for the elastic natural period, T_1 , of the target structure. IDA is performed by gradually increasing the magnification of the scaled ground motion group. On the other hand, T_1 is not dominant to the response in the SIBs targeted here. The equivalent period evaluated from equivalent stiffness based on the response deformation is used. However, in this paper, since the behavior from the plastic region to the hardening of NRBs is targeted, the equivalent period cannot be unambiguously determined. Therefore, like Nakazawa et al., the seismic isolation period, T_f , obtained from the horizontal stiffness of only NRBs is focused. T_f is a representative index indicating the performance of SIB [3].

The scaling uses velocity response spectrum, S_v , when damping factor is 0.05. The scaling is that the median of $S_v(T_f)$ on ground motion group matches to 100 cm/s. Fig. 6 shows velocity response spectrum after scaling. With the scaled ground motion group set to 1.0 times the standard, the acceleration magnification is increased from 0.1 to 7.5 times in increments of 0.1. For comparison, IDA using the notification wave shown in Table 2 is also performed. Fig. 7 shows velocity response spectrum of the notification wave after scaling.

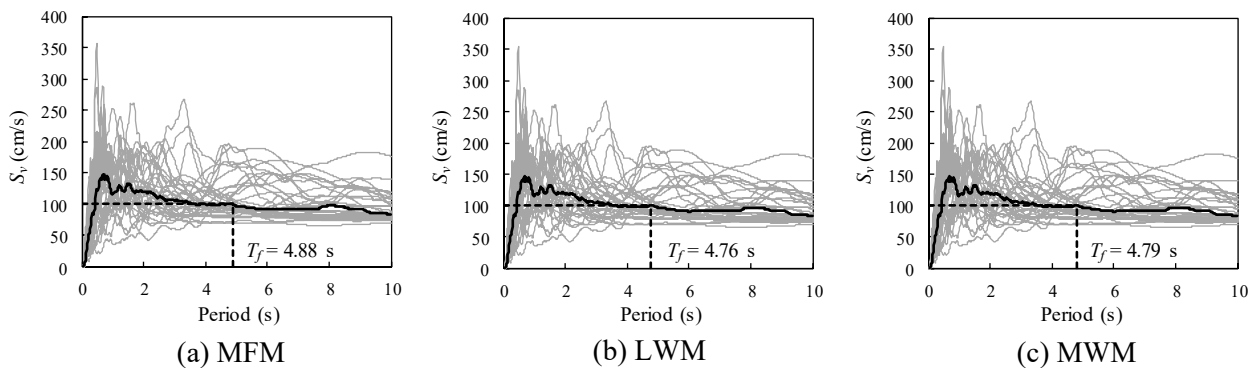


Fig. 6 – Velocity response spectrum, S_v , after scaling

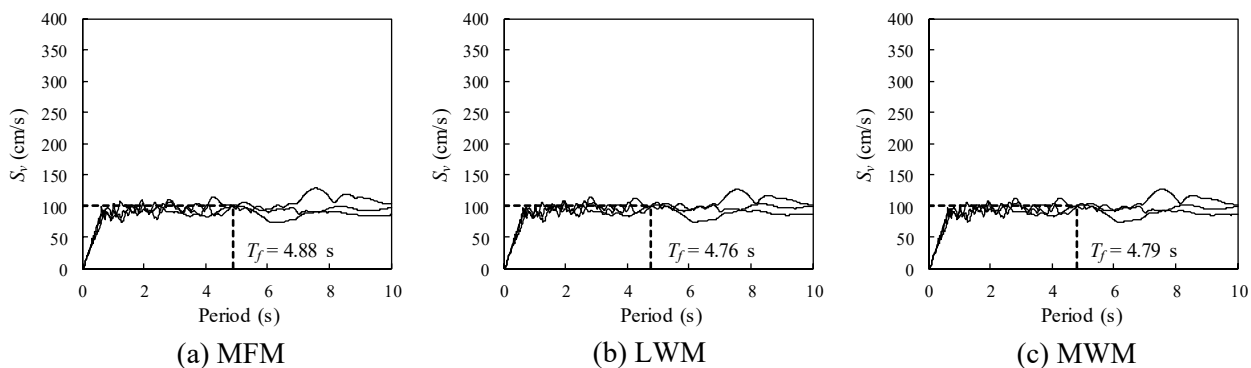


Fig. 7 – Velocity response spectrum, S_v , of the notification wave after scaling



4. Incremental Dynamic Analysis

4.1 Incremental Dynamic Analysis Result

Fig. 8-10 shows the median of maximum relative displacement, D_i , the median of maximum inter-story drift angle, R_i , and the median of maximum ductility factor, μ_i , by IDA respectively. The ground motion magnification is between 1.0 and 2.5. The ground motion magnification is plotted as 1.0, 1.5, 2.0, and 2.5, and the other are indicated by solid lines. In MFM, R_i and μ_i of the superstructure concentrates in the lower story as ground motion magnification increases. R_i and μ_i increase rapidly when a certain ground motion magnification is exceeded. In LWM, the deformation concentration in the lower story is suppressed. However, when a certain ground motion magnification is exceeded, the deformation concentrates on the upper layers where the stiffness is relatively lower and thus increases rapidly. In MWM, the concentration of deformation is suppressed, and the deformation is effectively dispersed by the multi-story shear walls. In addition, at the same ground motion magnification, R_i and μ_i are smaller than those of MFM and LWM.

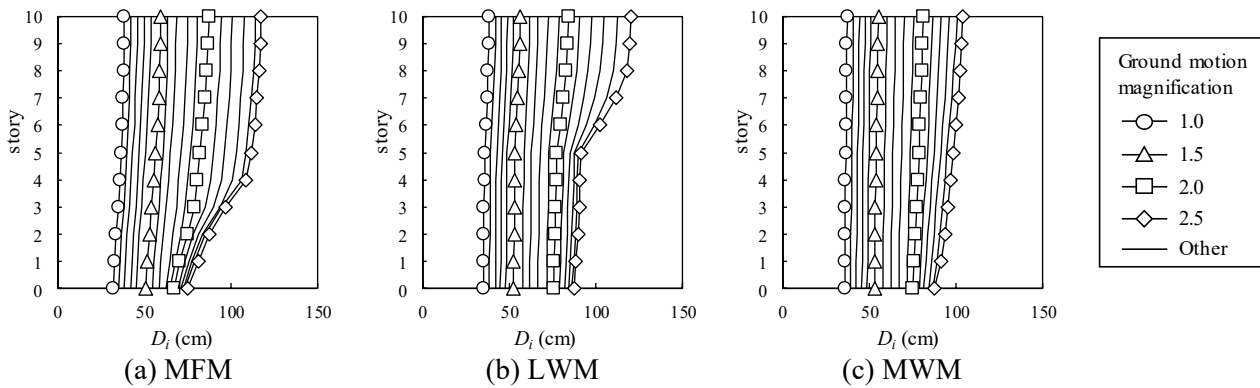


Fig. 8 – Median of maximum relative displacement, D_i

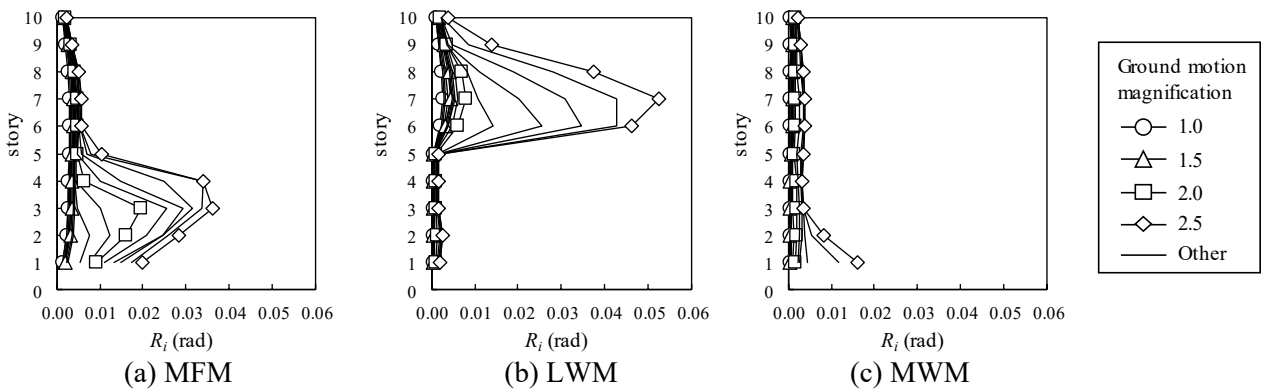


Fig. 9 – Median of maximum inter-story drift angle, R_i

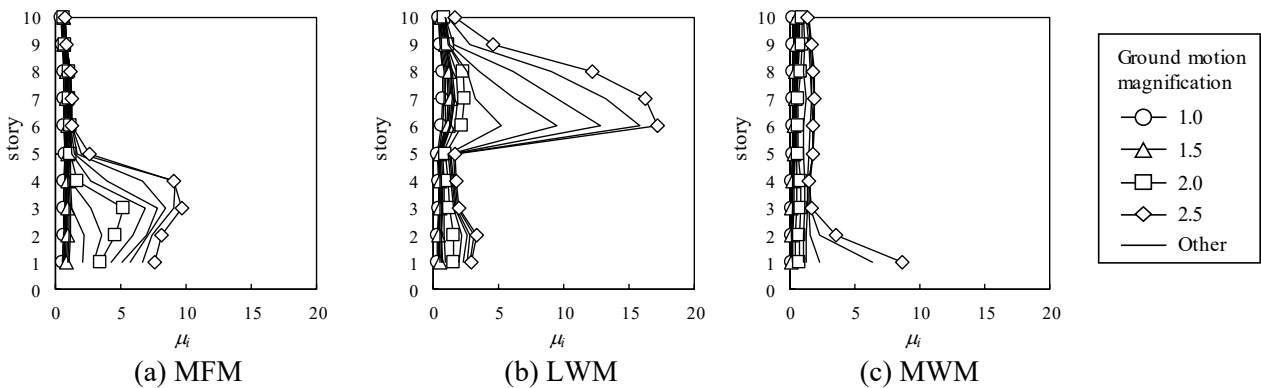


Fig. 10 – Median of maximum ductility factor, μ_i



Fig. 11 shows the deformation of the seismic isolation layer, δ_m , for the ground motion magnification. In (a) to (c), the results of each model for each ground motion are shown by solid gray lines, and the median is shown by solid black line. The results of the notification wave are shown by black broken lines. Fig. 11 (d) shows the median of each model in comparison. In MFM, from about 70 cm, which is the second stage of hardening, the median of δ_m for the ground motion magnification becomes gradual. In LWM and MWM, the median of δ_m increases similarly. From about 90 cm, the median of δ_m for the ground motion magnification becomes gradual. The median of δ_m of each model is about the same until the ground motion magnification is about 1.8. However, when the ground motion magnification exceeds that, the median of δ_m of LWM and MWM becomes larger than that of MFM.

Fig. 12 and 13 shows the maximum inter-story drift angle, R , and the maximum ductility factor, μ , for ground motion magnification respectively. R and μ indicate the largest of all layers. In all models, the median of R and μ increase rapidly beyond a certain ground motion magnification. The median of R and μ increase when ground motion magnification exceeds about 1.7 in MFM, about 2.0 in LWM, and about 2.3 in MWM. In MFM and LWM, R and μ increase similarly up to about 1.7 of ground motion magnification. When ground motion magnification exceeds that, the median of R and μ of MFM are larger than those of LWM at the same ground motion magnification. However, the increase rate of median of R and μ for ground motion magnification are larger in LWM than in MFM. Therefore, when the ground motion magnification is about 2.2, the median of R and μ is larger in LWM than in MFM. At the same ground motion magnification, the median of R and μ is smaller in MWM than in MFM and LWM.

In Fig. 11-13, according to the IDA results by the notification waves, the ground motion magnification for the same response value increases in the order of JMA-Kobe 1995 NS phase, Random phase, and Hachinohe 1968 NS phase. The response value by the notification wave of Hachinohe 1968 NS phase is almost the same as the median of response value by the ground motion group. The result from the notification wave is more conservative than the median value of the ground motion group. These trends do not depend on the analytical model of the superstructure.

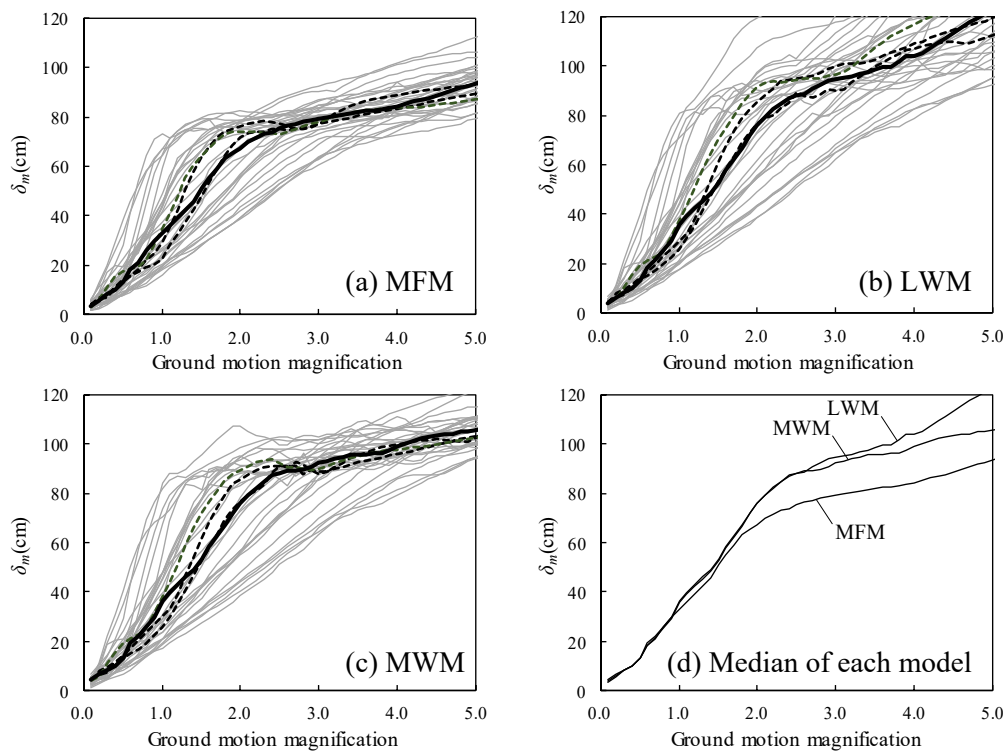


Fig. 11 – Maximum Deformation of seismic isolation layer, δ_m , for ground motion magnification

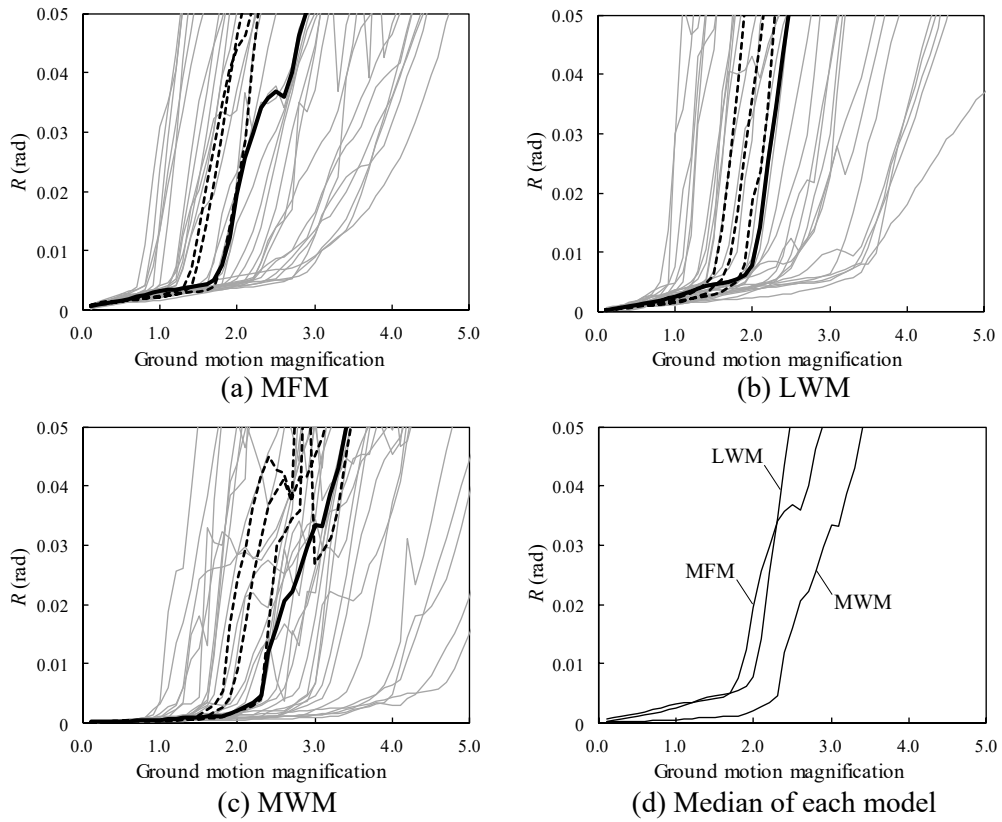


Fig. 12 – Maximum inter-story drift angle, R , for ground motion magnification

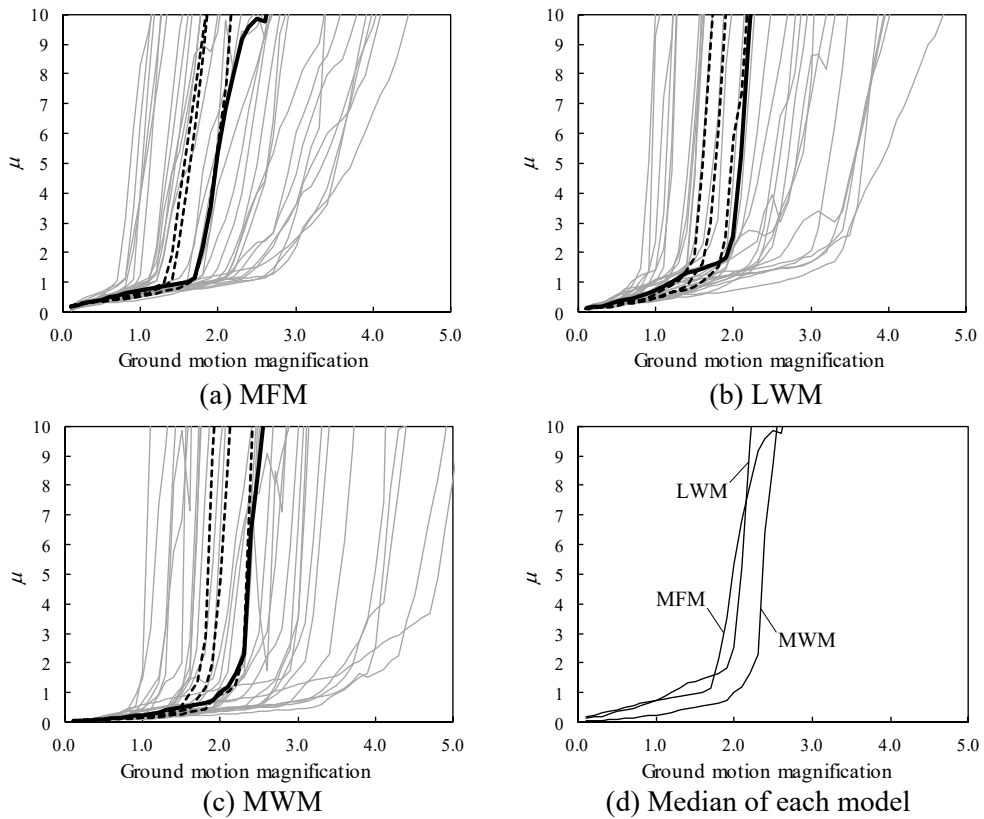


Fig. 13 – Maximum ductility factor, μ , for ground motion magnification



4.2 Fragility Curve and Safety Margin Ratio

Fig. 14 shows an example of fragility curve for limit value. Here, the deformation of the seismic isolation layer is 60 cm as limit value in MFM. In SIBs of Japan, it is a common value to set the moat wall clearance to 60 cm. Counting the number of ground motions that exceed the limit value for the ground motion magnification on the horizontal axis in Fig. 11-13, the fragility curve is obtained as a cumulative distribution function of a lognormal distribution. The plot in Fig. 14 shows the cumulative value of the ground motion that the deformation of the seismic isolation layer exceeds 60cm, and the solid line is the fragility curve. The intersection of the dashed line and the fragility curve indicates the ground motion magnification that reaches the limit value with a probability of 50%, and this ground motion magnification is defined as the safety margin ratio (SMR) in this paper.

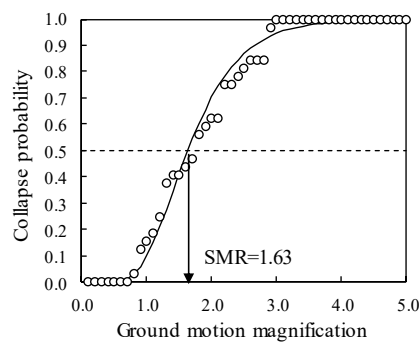


Fig. 14 – Fragility Curve

Fig. 15 shows the fragility curves of each model when the deformation of the seismic isolation layer, δ_m , the maximum inter-story drift angle, R , and the maximum ductility factor, μ , are used as the limit values. As the limit values, δ_m is 60 cm, R is 1/100, and μ is 2.0. When designing a high-rise building in Japan, the maximum inter-story drift angle 1/100 and the maximum ductility factor 2.0 are standard values as design criteria for extremely rare ground motions. In this paper, the limit value for the superstructure of SIBs is set these.

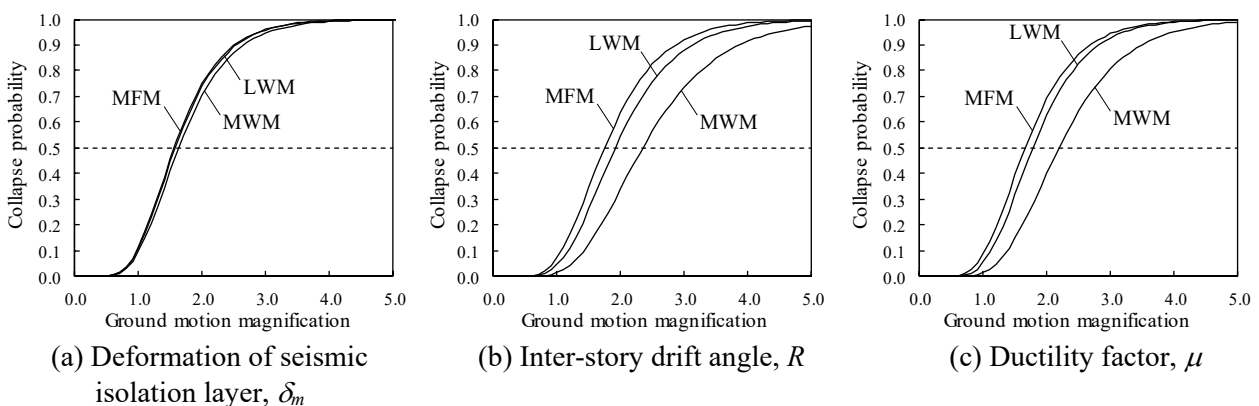


Fig. 15 – Fragility Curve

The fragility curves of each model are similarly when δ_m is set at 60 cm as limit value. When R is set at 1/100 as limit value, the fragility curve moves to the right in the order of MFM, LWM, and MWM, and SMR is improved. The same applies to the tendency when μ is set at 2.0 as the limit value.

Fig. 16 shows SMR of each model. SMR is the same value for each model when δ_m is set at 60 cm as limit value, which is about 1.6. When R and μ are set at 1/100 and 2.0 respectively as the limit values, SMR



are larger in the order of MFM, LWM, and MWM. SMR is more than 2.0 in MWM. In MFM, SMR at each limit value is about 1.7, which is a similar value. In LWM and MWM, SMR with $R=1/100$ and $\mu=2.0$ as the limit values is larger than the case where δ_m is set at 60 cm. The difference is larger in MWM. Therefore, if large deformation of seismic isolation layer is acceptable, it is effective for improving the safety margin to arrange the seismic elements in the entire building in a well-balanced manner like MWM.

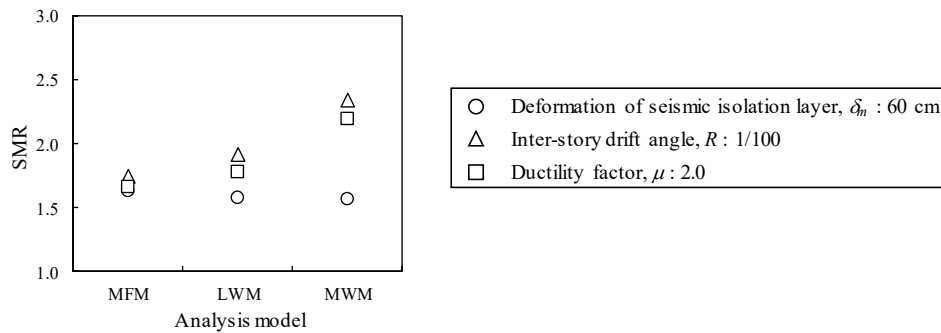


Fig. 16 – SMR for analysis model

5. Conclusion

This paper shows that the safety margin of SIBs against extreme ground motions is evaluated by IDA. The effect of the difference of the superstructure models on the safety margin of SIBs is analyzed. The results are as follows; 1) As ground motion magnification increases, in MFM and LWM, deformation concentrates on the lower and upper layers respectively, and increases sharply when a certain ground motion magnification is exceeded. In MWM, the concentration of deformation is suppressed, and the multi-story shear wall effectively disperses the deformation. 2) When the deformation of the seismic isolation layer is set to 60 cm as limit value, SMR becomes the same value for each model. When the maximum inter-story drift angle 1/100 and the maximum ductility factor 2 are the limit values, SMR increases in the order of MFM, LWM, and MWM. 3) If large deformation of seismic isolation layer is acceptable, it is effective for improving the safety margin to arrange the seismic elements in the entire building in a well-balanced manner like MWM.

Acknowledgements

This work was supported by JSPS KAKENHI Grant Number JP17K06658. The authors also thank PEER for kindly allowing us to use the recorded earthquake data.

References

- [1] Kikuchi M, Black CJ, Aiken ID (2008): On the response of yielding seismically isolated structures. *Earthquake Engineering & Structural Dynamics*, **37**, 659-679.
- [2] Qu Z, Kishiki S, Nakazawa T (2013): Influence of Isolation Gap Size on the Collapse Performance of Seismically Base-Isolated Buildings. *Earthquake Spectra*, **29** (4), 1477-1494.
- [3] Nakazawa T, Kishiki S, Qu Z, Wada A (2012): Safety Margin Ratio-Based Design of Retaining Wall Clearance for Base-Isolated Structures. *Journal of Structural and Construction Engineering (Transaction of AIJ)*, **77**, 1159-1165. (in Japanese)
- [4] Higashino M, Okamoto S (2006): *Response Control and Seismic Isolation of Buildings*, Taylor & Francis, London and New York.
- [5] Architectural Institute of Japan (AIJ) (2013): *Recommendation for the Design of Seismically Isolated Buildings*.
- [6] Federal Emergency Management Agency (FEMA) (2009): *Quantification of Building Seismic Performance Factors*, Report No. FEMA P695.